Charge Density Analysis of Triplet and Broken Symmetry States Relevant to Magnetic Coupling in Systems with Localized Spin Moments

H. Chevreau,[†,‡] I. de P. R. Moreira,[†] B. Silvi,[‡] and F. Illas*[,†,‡]

Departament de Química Física i Centre de Recerca en Química Teòrica, Universitat de Barcelona, C/Martí i Franquès 1, E−08028 Barcelona, Spain, and Laboratoire de Chimie Théorique, Université Pierre et Marie Curie, 4 Place Jussieu, 75252 Paris-Cedex 05

Received: July 7, 2000; In Final Form: November 21, 2000

Comparison of electron charge density for triplet and broken symmetry solutions obtained from different computational methods together with the atoms-in-molecules (AIM) and electron localization function (ELF) topological analyses support the description of these systems through the Heisenberg Hamiltonian. The reduction of the low-energy spectrum to a purely spin Hamiltonian holds for all studied methods, although local density approximation (LDA) exhibits some noticeable deviation. The analysis of charge difference density plots clearly shows that the failure of LDA to describe magnetic coupling is due to the too-strong delocalization that leads to a qualitatively incorrect electron density in the region near the nuclei. Gradient-corrected and hybrid functionals correct this defect but in an exaggerated way. The role of mixing Fock exchange is also discussed.

I. Introduction

Magnetic coupling in several materials is important in various technological applications ranging from molecular magnets[1,2] to high-T_c superconductors[3]. Recent advances in ab initio configuration interaction methods[4,5] have finally allowed researchers to reach a quantitative understanding of magnetic coupling in compounds ranging from inorganic binuclear complexes[6−10] to several ionic solids including highly symmetric compounds,[11−15] Jahn−Teller distorted solids,[16−18] ladder compounds,[19] and a variety of superconductor parent compounds.[20,21] In the configuration interaction approach the magnetic coupling constant, J_{ij}, entering into the definition of the Heisenberg Hamiltonian

$$\hat{H} = -J_{ij}\,\hat{\mathbf{S}}_i\hat{\mathbf{S}}_j \qquad (1)$$

describing the spectrum arising solely from interactions between total net spin S_i and S_j, is obtained as the energy difference between the appropriate spin eigenfunctions. In principle, for a solid with localized spin moments it is necessary to include the summation over different neighbors and account for the infinite nature of the system. However, the magnetic coupling constant has been shown to be a local property involving only the interacting centers[22] and, hence, a local or cluster model approach can still be used to obtain accurate values of the magnetic coupling constant by means of configuration interaction wave functions.[23] For systems with a total spin of 1/2 per magnetic center, it is readily apparent that J_{ij} is simply given by the singlet−triplet difference and the choice of the sign in eq 1 is such that J_{ij} is positive for a ferromagnetic interaction favoring parallel spins. A mapping procedure can be used for more complex systems to establish a one-to-one correspondence between the eigenstates of the Heisenberg and exact, nonrelativistic Hamiltonians.[11,15,24]

Despite the remarkable success of the methods based on configuration interaction applied to magnetic coupling, there are many interesting systems that cannot be studied by this approach because of the large size of the systems. Inorganic binuclear complexes with voluminous ligands belong to this category. Similarly, the description of the electronic structure of ideal solids by means of a periodic approach precludes the use of configuration interaction wave functions. The common approach to these large systems relies on using a single Slater determinant to describe the electronic density of the system of interest. Clearly, such a choice does not always permit dealing with spin eigenfunctions. This is particularly true for the open-shell singlet relevant to magnetic coupling. Nevertheless, in some cases, it is possible to indirectly approximate the energy of the singlet by means of the so-called broken symmetry approach; this will be discussed in some detail in the next section.

II. An Overview of the Broken Symmetry Approach

The broken symmetry approach to open-shell singlet wave functions and related multiplets has long been used in the framework of unrestricted Hartree−Fock (UHF) calculations and in the primitive versions of density functional theory (DFT), such as Xα-scattered wave methods. In fact, it is often ignored that the first attempt to compute singlet−triplet splittings through the Xα-scattered wave method was reported about 25 years ago by Bagus and Bennett[25] and extended shortly afterward by Ziegler et al.[26] The broken symmetry approach to magnetic coupling was suggested by Noodleman,[27−30] initially also in the framework of Xα, and later Yamaguchi et al.[31−34] made significant contributions in the application of UHF to magnetic coupling. On the other hand, the broken symmetry approach is the commonly used procedure in solid-state physics, although it is often referred too as the spin-polarized approach. In this case, the magnetic coupling constant is obtained from energy

* Corresponding author. E-mail: f.illas@qf.ub.es
† Universitat de Barcelona.
‡ Université Pierre et Marie Curie.

10.1021/jp002453w CCC: $20.00
Published on Web 03/17/2001

differences between ferromagnetic and several antiferromagnetic (within the relevant supercells) solutions. (See, for instance, refs 24 and 35.)

Because the broken symmetry approach does not lead to a pure singlet wave function (or to a density derived from a singlet wave function), it is necessary to relate the expectation value of the energy of the broken symmetry solution to that of the pure singlet. For a system with two magnetic centers with spins S_1 and S_2, it has been shown that the energy of the broken symmetry (BS) state is a weighted average of the energies of the pure spin multiplets.[29,36,37] In the particular case of spin 1/2 magnetic centers, it is easy to show that the energy difference between the high-spin solution, which approximates the triplet state, and the BS solution, which approximates the open-shell singlet, is just half the singlet−triplet difference. This relationship is almost exact in UHF provided there is no significant overlap between alpha and beta spin orbitals.[37] In DFT there is no direct way to prove that this is also the case, although there are several indirect arguments that strongly suggest that the arguments above also hold in density functional calculations within the broken symmetry approach.[24] The mapping between Ising and exact Hamiltonians permits the derivation of these relationships in an elegant way.[15,24] In cases where the magnitude of the overlap between alpha and beta orbitals in the BS solution cannot be ignored, it is always possible to explicitly compute this value according to reported methods[27−30,37] or to estimate it using some of the procedures reported recently.[38,39]

Nevertheless, it is important to point out that other authors hold a point of view that differs substantially from the discussion above. It is possible to claim that the lowest energy obtained for a Kohn−Sham determinant with zero total z-component of the total spin is a good approximation of the energy of the lowest singlet state. Ruiz et al.[40−43] suggested that accurate values of the magnetic coupling constant of transition metal dinuclear complexes can be obtained by using the hybrid B3LYP exchange-correlation functional[44,45] and by considering that the energy of the broken symmetry solution is that of the lowest singlet. Despite the impressive numerical results, there are many serious arguments against this point of view which suggest that one may have the right answer for the wrong reason.[24] In particular, it is worth pointing out that in organic biradicals, agreement with experiment within B3LYP is only achieved when considering that the broken symmetry energy lies halfway between singlet and triplet[24,46] (vide infra). This is in line with the work of Martin and Illas on transition metal ionic solids.[47,48] They show that the magnetic coupling constant strongly varies with the choice of the exchange-correlation functional and, in particular, with the amount of Fock exchange included. To conclude this discussion, it is worth mentioning that local density approximation (LDA) is usually used in solid-sate physics to derive magnetic properties of strongly correlated systems. This is surprising because it is well-known that LDA incorrectly describes such compounds as metals, thus resulting in unphysically large values for the magnetic coupling constant of these materials.[49−51]

The discussion above reflects the difficulties faced by present exchange-correlation functionals to properly describe the magnetic coupling mechanisms on several systems. The development of new functionals that may overcome these difficulties requires a detailed study of the density obtained from different possible choices. In particular, it is necessary to better understand the role played by hybrid functionals that mixes a part of Fock exchange with the local or gradient-corrected functional. This mixing seems to be the clue for the success of the density functional description of magnetic coupling in organic biradicals[46] and also on transition metal compounds,[47] although different mixtures are required in each case. In this work we present several analyses of the charge density for the triplet and BS states that are relevant to magnetic coupling of systems with total 1/2 spin moments. This analysis is performed for a variety of computational schemes and includes the comparison with the exact solution for a model system. The analysis is based on plots of the total charge density, of the charge density analysis topology in the sense of the atoms-in-molecules (AIM) theory,[52] and on the topology of the electron localization function (ELF) introduced by Becke and Edgecombe[53] and extensively used to analyze the chemical bond in various situations.[54−57]

III. Model Systems and Computational Details

In this work the analysis of electronic charge density for triplet and BS solutions is conducted for three representative systems that have previously been used in work concerning different aspects of this problem.[37] The charge densities of different systems have been obtained by using nonrelativistic quantum chemical methods. Therefore, spin polarization terms arising from spin−orbit, hyperfine, or higher order interactions are not taken into account. The first system is H−He−H with d(H−He) = 1.675 Å for which the system exhibits an antiferromagnetic character. The choice of this model system comes from the need to compare to exact values whenever possible and the fact that full configuration interaction solutions for triplet and singlet can be obtained and used as a reference for other computational methods. This model system has also been referred to by many different authors.[34,36,37,43,58] The second system, $(Cu_2Cl_6)^{2-}$, is the archetype of binuclear complexes[1,2] and has also been studied in detail by configuraton interaction and broken symmetry approaches.[4,10,37] Finally, the third system is the high-T_c superconductor parent compound La_2CuO_4, or more appropriately an embedded Cu_2O_{11} model representation of this material. This system is representative of strongly correlated systems, a family of compounds that are not well described at all by means of LDA.[49−51] In fact, a proper description of magnetic coupling in these systems requires hybrid exchange-correlation functionals with ∼50% nonlocal Fock exchange.[47,48] Structural data and geometries for $(Cu_2Cl_6)^{2-}$ and Cu_2O_{11} are those previously used in ref 37. All calculations are performed using exactly the same Gaussian basis sets that were used in ref 37. Because the main goal of this paper is the topological analysis of charge densities, we deliberately omitted reporting numerical values for the magnetic coupling constant and other relevant quantities. Most of these values have already been given in ref 37 so that only new pertinent results are included here.

Several analyses of the triplet and BS densities obtained by different electronic structure methods have been performed. The different electronic structure methods are UHF and various density functional approaches beginning with LDA and including the BLYP gradient-corrected exchange-correlation functional which combines Becke's exchange[59] and the correlation functional by Lee et al.[45] The B3LYP[44,45] and B3PW91[44,60] hybrid functionals have also been explored. These hybrid functionals combine different mixtures of Becke and Fock exchange functionals and were introduced initially by Becke to reproduce the thermochemistry of a variety of organic molecules.[44] Different hybrid functionals have also been proposed during the past few years.[61−65] It is always possible to find a given mixing that optimizes a particular property at the expense of

others. In particular, the density functional description of magnetic coupling in biradicals, with magnetic orbitals essentially of s and p character, is very different from the one corresponding to magnetic coupling in transition metal compounds, with magnetic orbitals essentially of d character.[24] In the former, B3LYP performs reasonably well,[46] whereas a larger amount of Fock exchange is needed in the later.[47,48] Therefore, to avoid an unnecessary large set of functionals we decided to explore just different mixtures of Becke and Fock exchange that will be denoted as B(X)LYP, where X stands for the percent of Fock exchange; X = 0 will lead to BLYP and X = 100 to FLYP. The first analysis concerns density difference plots for triplet and BS solutions obtained from a given method. The next point also involves density differences but for the BS solution obtained using different methods. The analysis of density differences is complemented by topological analysis based on the AIM theory[52] and on the ELF function.[53−55]

The final Kohn−Sham orbitals have been obtained by means of the Gaussian98 suite of quantum chemistry programs.[66] Next, the TopMoD code[67] has been used to obtain the electronic charge densities from the Kohn−Sham orbitals and to perform the AIM and ELF topological analysis.

IV. Basics of AIM and ELF Topological Analysis

Both AIM and ELF methods use a topological analysis to define atoms or bonds in a molecule by partitioning a given function in the real space. The maxima of a given local function define attractors, and the set of points connected to the same maximum defines a basin. In the early seventies, Bader suggested use of the topological analysis of electronic density.[52] In this case the attractors are located at the nuclei and their basins are analyzed in a chemical sense as atoms-in-molecules. It is then possible to associate properties of each atom, such as its population defined as the integration of $\rho(r)$ over a given basin. The introduction of a bonding path permits definition of the existence of a bond between two atoms.

The choice of the electron density as the function subject to topological analysis is not the only chemically meaningful possibility. It is also possible to perform the analysis of the electron density of an electron pair much in the spirit of the definition of chemical bond according to the well-known Lewis structures. Becke and Edgecombe introduced the ELF or η, as

$$\eta(\mathrm{r}) = \frac{1}{1 + \left(\frac{D}{D_0}\right)^2} \tag{2}$$

where D is a measure of the excess of total kinetic energy resulting from Pauli repulsion[55] and D_0 is the kinetic energy for an homogeneous electron gas of the same density. Within this definition, the ELF function is limited to the [0,1] interval and the upper limit stands for a high localization. The ELF topological study provides additional insight to the AIM description because it allows us to distinguish between core and valence electrons and, in this last case, between lone pairs, V(X) for an atom X, covalent bond, V(X,Y), between atoms X and Y, or multicentered bonds. The mechanisms of magnetic coupling are very sensitive to the electronic density of the bridging ligands. Therefore, it is expected that ELF topological analysis can provide important information about the similarities and differences between triplet and BS densities and between different computational methods.

V. Structural Stability and Spin Polarization

In the absence of any external magnetic field, the Hamiltonian commutes with the total square spin operator. Hence, the total spin is a good quantum number and all states have a definite multiplicity. However, in the presence of an external magnetic field, the resulting Hamiltonian commutes with the component of total spin operator in the direction of the field only. The low-energy states will now correspond to the spin-polarized ferromagnetic and antiferromagnetic solutions. Here, spin polarization appears as a consequence of the external magnetic field. In this section we will show that this result can also be anticipated from the theory of gradient dynamic systems. In addition, we will use these topological arguments to discuss the reduction of the low-energy spectrum to that predicted by the Heisenberg Hamiltonian.

In fact, the direct space description of the chemical bonding as introduced in the AIM[52] and in the ELF[54−57] approaches relies on the mathematical theory of dynamical systems[68,69] and more particularly on the gradient dynamical systems bounded in the euclidean space R^3. A gradient dynamical system is the vector field obtained by applying the gradient operator to a function defined as continuous and derivable in all points of a given manifold, here R^3. This function, referred to hereafter as potential function and noted by $V(r:\{\alpha_i\})$, depends on a set of $\{\alpha_i\}$ parameters that form the control space. A gradient dynamical system is characterized by its critical points which are the points $\mathbf{r}_c$ where $\nabla V(\mathbf{r}_c:\{\alpha_i\}) = 0$. There are different types of critical points defined by its index, that is, the number of positive eigenvalues of the potential second derivative matrix (the Hessian matrix) calculated at $\mathbf{r}_c$. The number and the type of critical points are constrained by a phase-like rule, the Poincaré−Hopf formula

$$\sum_P (-1)^{I_P} = \chi(M) \tag{3}$$

where I_P stands for the index of the critical point P and $\chi(M)$ for the Euler characteristic of the manifold. A critical point is said to be hyperbolic if none of the eigenvalues of the Hessian matrix is zero. An important property of the dynamical systems is the *structural stability* investigated by Peixoto[70] and by Palis and Smale.[71] A dynamical system is structurally stable if any infinitesimal perturbation leaves its critical points unchanged in number and type. A necessary condition for structural stability is that all critical points are hyperbolic. The gradient dynamical system of a potential function used to describe a stable physical system should be structurally stable, whereas metaestable systems imply structural instability. As examples in physical chemistry we mention the explanation of the deviation from the jellium model of the interstitial electronic density in metals[72] or the predictive rules for the protonation sites in bases.[73]

The structural stability can be also invoked to interpret the phenomenon of spin polarization. Let us first consider a molecular system with two open shells as those described above for the study of magnetic coupling. In the triplet state, the component with total $S_z = 0$ gives rise to a uniformly null spin density, that is, $\rho^\alpha(\mathrm{r}) - \rho^\beta(\mathbf{r}) \equiv 0$. Therefore, the dynamical system of the spin density is structurally unstable because any point of the molecular space is a nonhyperbolic critical point. As a consequence, any small perturbation due to the interaction with an external magnetic field will stabilize the $S_z = \pm 1$ components for which the spin density is not uniform and the three triplet components will no longer be degenerated. The situation is similar for the open-shell singlet because the spin density is identically zero in the absence of an external magnetic field. The removal of the constraint of the wave function to be a spin eigenfunction stabilizes the spin-polarized solution that corresponds to a structurally stable gradient field of the spin

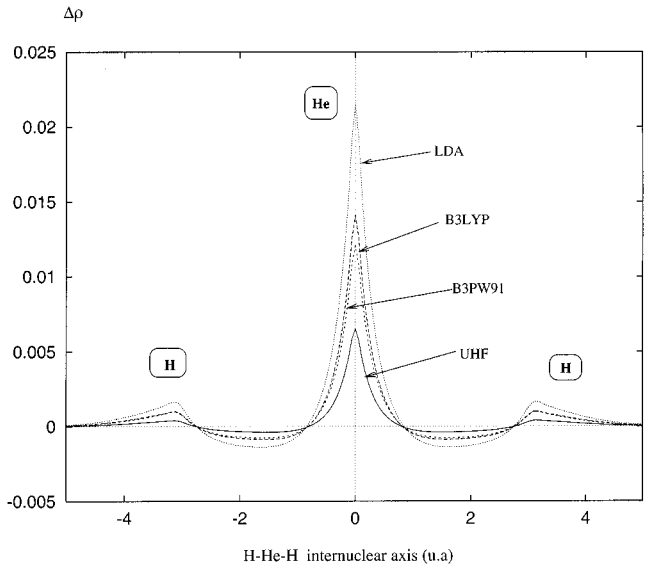

Figure 1. Difference of charge electron density [in atomic units (au)] for the triplet and broken symmetry solutions of the H−He−H model system as obtained from different computational methods.

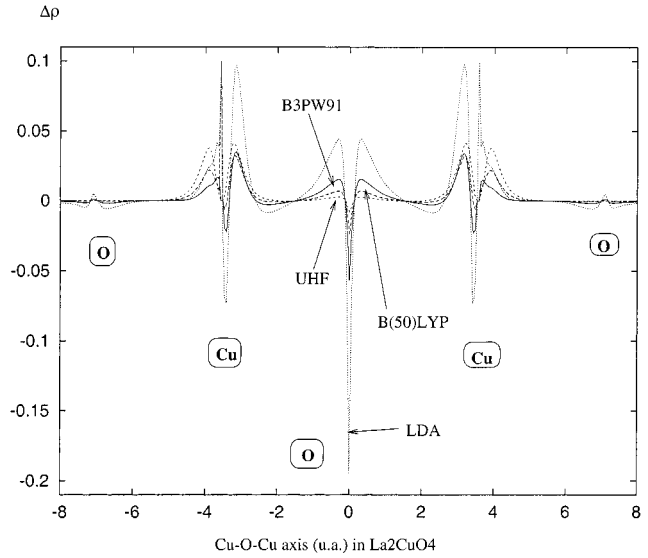

Figure 2. Difference of charge electron density (in au) for the triplet and broken symmetry solutions of the Cu_2O_{11} cluster model representation of La_2CuO_4 system as obtained by different computational methods.

density function. Therefore, spin polarization in the presence of vanishing but nonzero external magnetic field can be regarded as a consequence of the structural instability of the spin density function.

On the other hand, for other potential functions such as ELF, the transition from the nonpolarized to the polarized spin states is felt as a weak perturbation that leaves the gradient field topology constant provided it is structurally stable in the initial state. In the forthcoming discussion we will show that this is indeed the case and, as a consequence, the charge density and its topology remain almost the same from the triplet to the broken symmetry solution and the systems behave according to the Heisenberg Hamiltonian.

VI. Results from Electronic Charge Density Difference Analysis

The reduction of magnetic coupling to a pure spin problem governed by the Heisenberg Hamiltonian (cf. eq 1) is based on the assumption that high and low spin states do only differ in the total spin coupling and, hence, share the same total density. Ab initio calculations of magnetic coupling in systems with total spin larger than 1/2,[8−15] thus presenting various low-lying electronic states related to magnetic coupling, show that the low-energy spectrum of this system is in agreement with that derived from the Heisenberg Hamiltonian. This is an indirect proof of the reduction mentioned above. A more straight comparison is provided by the direct comparison of electronic charge densities corresponding to the triplet and BS solutions and by the corresponding topological analysis (vide infra). For the H−He−H model system, Figure 1 presents electronic charge density differences obtained by several computational methods. The plot is along the internuclear axis and includes the "bridging" ligand, which is an important region of space concerning superexchange-related mechanisms. This plot already shows an important result: the density differences are almost insignificant. (Notice the small values in the ordinate axis.) A second important result concerns the differences between different methods. The smallest difference between triplet and BS densities correspond to UHF and the largest to LDA, with the hybrid B3LYP and B3PW91 lying somewhere in between. The same description is obtained for both $(Cu_2Cl_6)^{2-}$ and Cu_2O_{11},

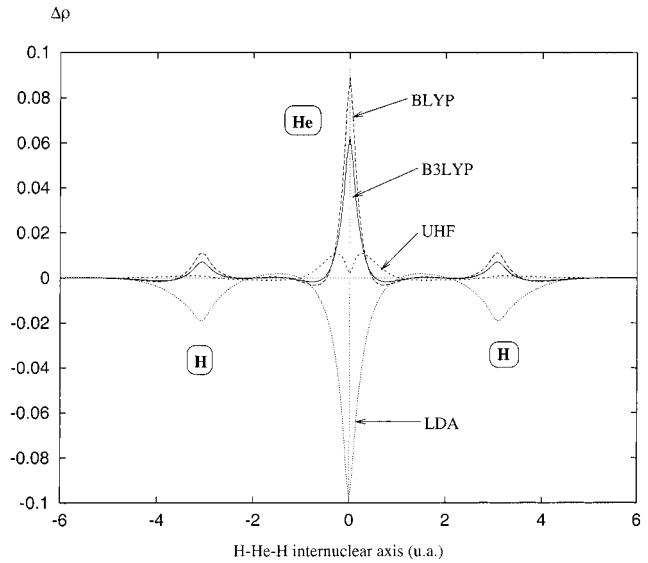

Figure 3. Difference of charge electron density (in au) corresponding to the broken symmetry solution of the H−He−H model system as obtained from a given method and that obtained from the exact FCI singlet wave function.

although the density differences are somewhat larger, especially for LDA. The results for Cu_2O_{11} are reported in Figure 2. Henceforth, the analysis of triplet and broken symmetry densities reveals that these systems do indeed follow the behavior predicted by the Heisenberg Hamiltonian, the deviations being larger for LDA in all cases.

The largest deviation of LDA from the Heisenberg behavior is correlated with the largest deviation from the exact density, for the present basis set, obtained from a full configuration interaction (FCI) wave function. The difference density between a given method based on broken symmetry and the exact solution for the open-shell singlet of H−He−H is presented in Figure 3 for points along the internuclear axis. Here, the values on the density axes are somehow larger and the changes are noticeable. The UHF density is surprisingly close to the FCI one, and the LDA deviates the most. This deviation between the FCI singlet and the different BS solutions is also found when comparing the FCI triplet to the $M_s = 1$ unrestricted solution.

This is not at all an unexpected result, because this is effectively a Heisenberg system. The charge density difference between BS and triplet is almost zero and, hence, both deviate almost equally from the exact FCI solution. In addition, Figure 3 shows that LDA largely underestimates the electronic charge density in the region near the nuclei, especially on that corresponding to the bridging ligand. This large underestimation of electronic charge density in LDA reveals the tendency of this approach to delocalize the density in excess, thus resulting more in a metallic description than on a magnetic system. This is in agreement with the results arising from Figure 1 that show that LDA deviates considerably from a magnetic system with localized spins. Likewise, this result permits a better understanding of the failure of LDA to properly describe the electronic structure of NiO, La_2CuO_4, and other compounds[49−51] generally termed strongly correlated systems in the framework on solid-state physics. Gradient-corrected (BLYP) and hybrid (B3LYP) exchange-correlation functionals show a behavior that is the opposite of LDA. The exaggerated tendency of LDA to delocalize is reversed, but deviations from the exact density are smaller. In a way, gradient-corrected and hybrid functionals introduce changes in the electronic charge density that are in the right direction, but the corrections to LDA appear to be too large. Therefore, it is possible that the numerical success of some of the existing functionals relies, at least in part, on some sort of error cancellation. On the other hand, the closeness between UHF and exact densities supports the idea of several authors[74−77] to introduce electronic correlation effects through direct application of correlation functionals on the HF density according to the theorem of Levy.[78] The widely used correlation functional developed by Lee et al.[45] is based precisely on the earlier work of Colle and Salvetti with the correlation factor[75]. Unfortunately, the existing correlation functionals do not seem to be accurate enough and may fail to reproduce some interaction energies.[79] This is what prompted Gill et al.[80] to suggest that better numerical values can be obtained by swapping out the exact exchange and swapping in a local or semi-local exchange correlation energy. This has since become quite the standard practice.

The failure of present exchange-correlation functionals to properly describe magnetic coupling in transition metal compounds, except perhaps accepting that in density functional calculations the BS approach leads to a pure singlet state,[43] has been attributed to deficiencies in the exchange functional.[47,48] Martin and Illas have suggested that reasonable values of the magnetic coupling constant of strongly correlated systems can be obtained by increasing the contribution of the Fock exchange in the hybrid functionals. Comparing the exact density with that obtained by increasing the contribution of the Fock exchange allows us to investigate the effect of this mixing in the electronic charge density. Such a comparison is presented in Figure 4 for hybrid schemes that are generically termed B(X)LYP, where X stands for the amount of Fock exchange. Hence, X = 0 leads to the BLYP gradient-corrected functional and X = 100 to F-LYP or UHF plus the LYP correlation functional. Figure 4 permits us to understand the rather good numerical success of the functional proposed by Martin and Illas that includes just 50% of Fock exchange. Because, in this particular case, UHF provides the best approach to FCI, it is not surprising that increasing X leads to improvement in the total electronic charge density. However, the important message from Figure 4 is that the deviation of the density obtained from gradient-corrected and B3LYP or B3PW91 hybrid functionals with respect to the

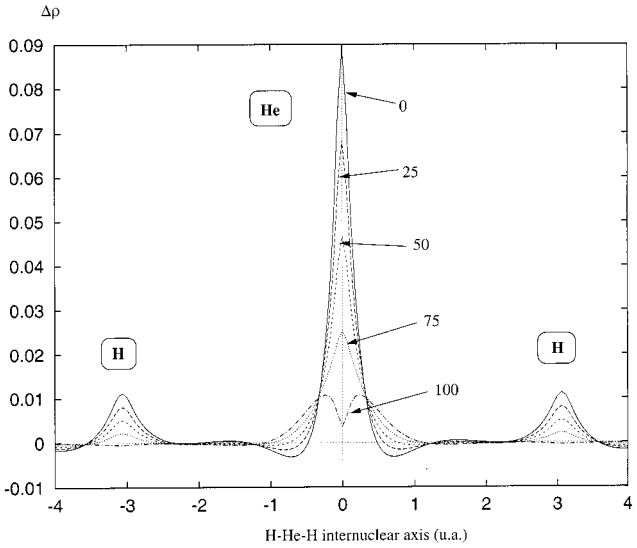

Figure 4. Difference of charge electron density (in au) corresponding to the broken symmetry solution of the H−He−H model system as obtained from an hybrid B(X)LYP scheme with X being the amount of Fock exchange and that obtained from the exact FCI singlet wave function.

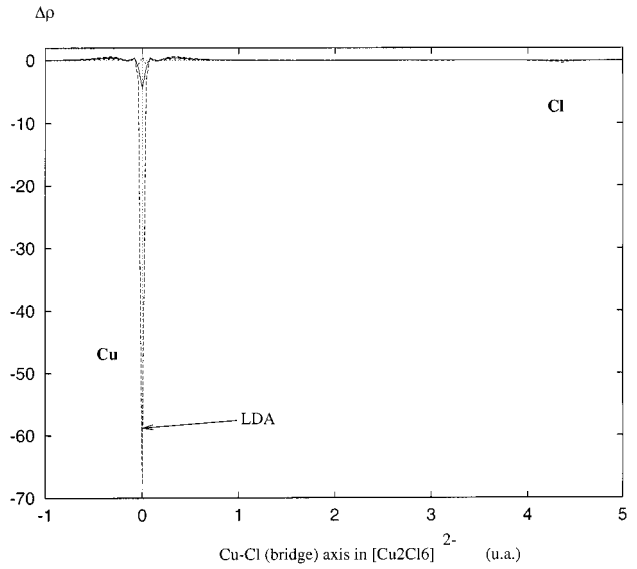

Figure 5. Difference of charge electron density (in au) corresponding to the triplet solution of the $(Cu_2Cl_6)^{2-}$ system as obtained from a given method and that from UHF.

exact value can be attributed to the exchange functional and supports the ideas of previous work in the same direction.[47,48]

Having discussed the H−He−H at length we now turn our attention to both $(Cu_2Cl_6)^{2-}$ and Cu_2O_{11} systems. In this case it is not possible to obtain the FCI density so the discussion is limited to comparison between approximate methods using UHF as the reference density. Because triplet and BS solutions lead to extremely similar densities, the forthcoming discussion is based on comparing electronic charge densities for the triplet state. The electronic charge density differences for $(Cu_2Cl_6)^{2-}$ is plotted along the line connecting the one Cu magnetic center and one Cl bridging ligand. Results are reported in Figures 5 and 6. Similarly, the electronic charge density of Cu_2O_{11} is plotted along the central Cu−O−Cu line. The electronic charge density differences are reported in Figures 7 and 8. The electronic charge density differences for both systems exhibit some remarkable figures. Notice the enormous difference between LDA and all other methods, especially near the

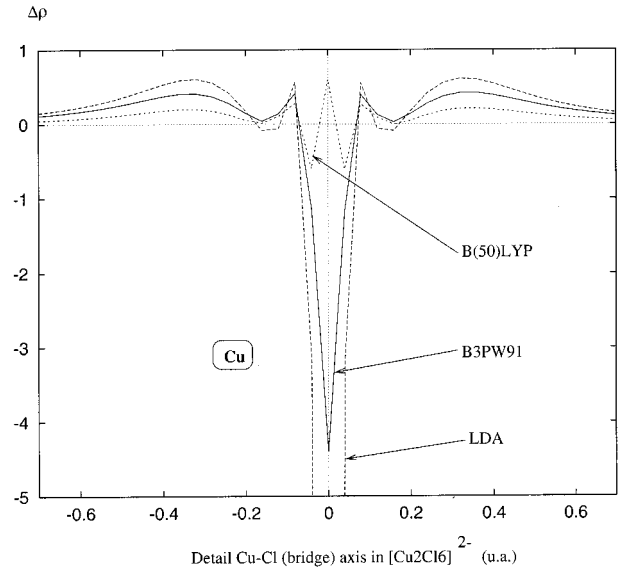

Figure 6. Detail of Figure 5 around a Cu atom.

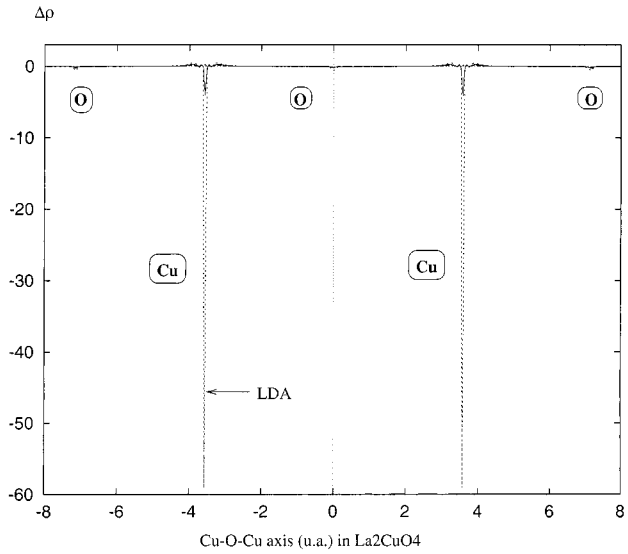

Figure 7. Difference of charge electron density (in au) corresponding to the triplet solution of the Cu_2O_{11}-cluster-model representation of La_2CuO_4 system as obtained from a given method and that obtained from UHF.

magnetic centers. The difference is so large that differences between different methods are only apparent if the scale is conveniently increased as in Figures 6 and 8. The exceedingly large deficit of density near the nuclei in LDA relative to all other methods is in agreement with the behavior already described by the H−He−H model system and fully supports the conclusions reached above. The most detailed plots in Figures 6 and 8 reveal considerable differences between UHF and the different hybrid functionals. The differences are even larger for gradient-corrected functionals, although much smaller than those found for LDA and are not reported in the figures. In the $(Cu_2Cl_6)^{2-}$ inorganic binuclear complex the magnetic coupling constant is really small,[81] and it is difficult to relate changes in the total electron charge density to changes in the magnetic coupling constant.

However, for La_2CuO_4 the situation is more transparent because of the rather large value of the magnetic coupling constant. Hence, in the Cu_2O_{11}-cluster-model representation of this compound, the largest differences in total charge density between UHF and other methods can be related to changes in

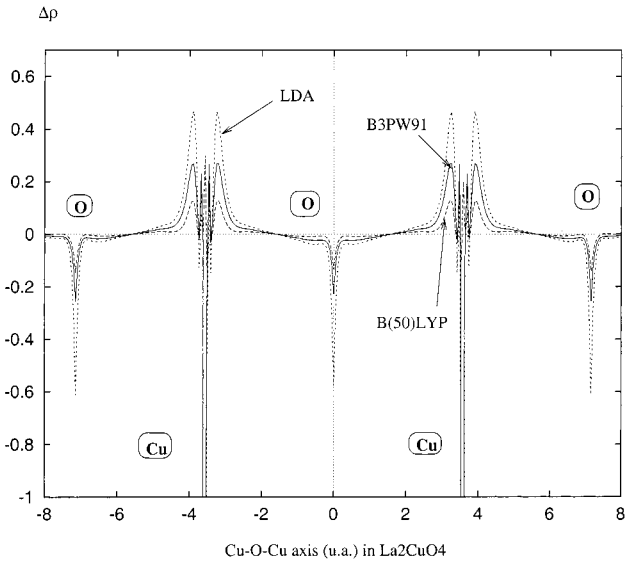

Figure 8. Detail of Figure 7.

the calculated coupling constant. The UHF value is 20−25% of the experimental value; LDA and gradient-corrected functionals predict values that are too large. The failure of LDA to properly describe the electronic and magnetic structure of La_2CuO_4 and related compounds has also been reported by several authors,[49,82] although LDA has generally been used to extract effective parameters for a more elaborate treatment.[83] Several approaches with different philosophies have been proposed to amend the LDA failure in describing highly correlated systems. Thus, LDA+U[84−87] and LDA+SIC[88,89] corrections to LDA have been reported from the field of solid-state physics, whereas hybrid DF approaches have been proposed from quantum chemistry. For this system, B3LYP is out by a factor of 2 and the B(50)LYP leads to a reasonable value. The electronic charge density difference plots in Figure 8 show significant differences in the density obtained by the different methods that are related to the calculated magnetic coupling constant. The difference between UHF and B(50)LYP is not very large but enough to change the calculated magnetic coupling constant by a factor of almost five.

VII. Results from AIM and ELF Topological Analyses

Both, AIM and ELF topological analyses were performed for H−He−H and $(Cu_2Cl_6)^{2-}$ systems. These analyses produced quite a large set of data concerning atomic and spin populations, fluctuations, and basin volumes. Restricting ourselves to the main results we first note that, within each method, the topology of the triplet and BS densities remains the same. Both differ through their spin densities only and not through their spatial localization. Accordingly, the perturbation induced by reversing one spin remains so local that it does not modify the surroundings supporting the reduction of the Hamiltonian to the Heisenberg form.

The ELF analysis of the triplet state electron density obtained by different methods reveals a rather interesting modification of the topology. When the calculated value of J increases, for example, from UHF to LDA, the bonding basins V(Cu,Cl) inside and outside the molecule tend to vanish and, simultaneously, the V(Cl) lone pairs get an excess of population. This effect is clearly seen when comparing Figures 9 and 10, which present a three-dimensional visualization of ELF as obtained from the UHF and LDA electron density, respectively. In terms of the ELF analysis the LDA description appears to be more ionic.

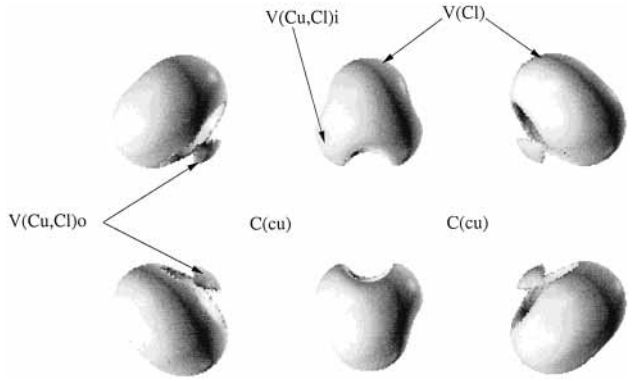

Figure 9. A 3D ELF visualization of the UHF triplet of $(Cu_2Cl_6)^{2-}$ from the molecular top view. The isosurface corresponds to ELF = 0.855 and C(Cu) denotes the Cu core basin, V(Cl) the Cl lone pairs, V(Cu, Cl) the bond between Cu and Cl. "i" represents the inside or bridging ligands, and "o" the outside ones. The C(Cl) cores are not visible with this view angle.

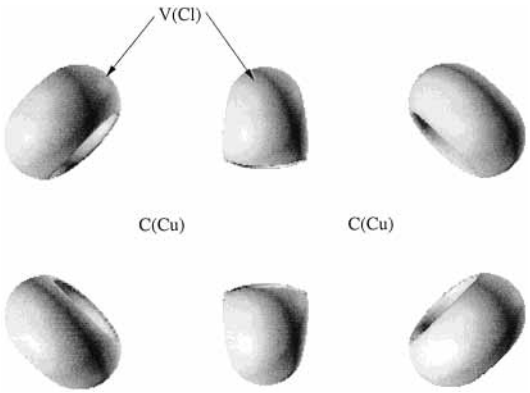

Figure 10. Same as Figure 9, but with ELF obtained from LDA.

This conclusion may seem to be paradoxical because the comparison of charge densities revealed that LDA tends to delocalize in excess the electron density out of the nuclei. However, the tendency of LDA to describe the systems as metallic includes the fact that increasing delocalization results in a decrease of the covalent contribution, and the loss in electron population in the bonding basin increases the population in the lone pairs. The electronic density flows to the molecular edge and delocalizes as much as possible. Hence, the ELF analysis of LDA is consistent with the comparison of charge densities in the previous section. This particular aspect of LDA is clearly seen in the ELF analysis only. The AIM analysis only shows a very small decrease of the population of the edge anions relative to the bridge ones that is larger than in any other method. This difference between AIM and ELF can be explained easily by looking at the position of the V(Cu,Cl) basins along the Cu−Cl line. These basins are very close to Cl just showing that Cl is the most electronegative atom. In AIM, the density corresponding to these bonding basins will be attributed largely to Cl; thus, a modification in the ELF population of the V(Cu,Cl) basin will be located mainly in the Cl atomic basins defined in the AIM analysis. Because these modifications do only affect the same atomic basin there are no noticeable differences in the AIM analysis.

VIII. Conclusions

The comparison of electron charge density for triplet and broken symmetry solutions obtained from different methods together with the AIM and ELF topological analyses supports the description of these systems through the Heisenberg Hamiltonian. The reduction of the low-energy spectrum to a purely spin Hamiltonian holds for all studied methods, although LDA exhibits some noticeable deviation. Likewise, for the H−He−H model system, the LDA electron charge density is the one that deviates most from the exact FCI and, surprisingly enough, UHF is the one that deviates least. The gradient-corrected and hybrid functionals correct the deficiencies of LDA in the right direction but into too large an extent. The B3LYP electron charge density for the broken symmetry solution deviates considerably from the exact values for the lowest singlet for this model system. Hence, the claim that the broken symmetry B3LYP density functional charge density is very close to that of the corresponding singlet state is not supported.

For the $(Cu_2Cl_6)^{2-}$ and Cu_2O_{11} systems, similar conclusions are found. LDA exceedingly delocalizes the electron charge density in the region near the nuclei and, hence, leads to values of the magnetic coupling constant that are too large. On the other hand, the comparison of total electron charge density and topology for different gradient-corrected and hybrid exchange functionals reveals significant differences. In particular, the use of gradient-corrected functionals corrects the deficiencies of LDA but too strongly. Introduction of Fock exchange tends to reduce these differences but there is no a priori way to decide the precise mixing required, in particular, to obtain reliable values of the magnetic coupling constant.

Acknowledgment. The authors are indebted to the DGICYT of the Ministerio de Educación y Ciencia of Spain (project PB98-1216-CO2-01) and to the CIRIT of the Generalitat de Catalunya (grant SGR99-40) for financial support. H.C. acknowledges support from the European Commission through the TMR network contract ERBFMRX-CT96-0079, Quantum Chemistry of Excited States. I. de P. R. M. is grateful to the University of Barcelona for financial support.

References and Notes

(1) Kahn, O. *Molecular Magnetism*; VCH: New York, 1993.
(2) Gatteschi, D., Khan, O., Miller, J. S., Palacio, F., Eds. *Magnetic Molecular Materials*; NATO ASI Series; Kluwer: Dordrecht, 1991.
(3) Dagotto, E. *Rev. Mod. Phys.* **1994**, *66*, 763.
(4) Miralles, J.; Daudey, J. P.; Caballol, R. *Chem. Phys Lett.* **1992**, *198*, 555.
(5) Miralles, J.; Castell, O.; Caballol, R.; Malrieu, J. P. *Chem. Phys.* **1993**, *172*, 33.
(6) Castell, O.; Caballol, R.; Garcia, V. M.; Handrick, K. *Inorg. Chem.* **1996**, *35*, 1609.
(7) Castell, O.; Caballol, R. *Inorg. Chem*. **1999**, *38*, 668.
(8) Mödl, M.; Povill, A.; Rubio, J.; Illas, F. *J. Phys. Chem. A* **1997**, *101*, 1527.
(9) Cabrero, J.; Ben Amor, N.; de Graaf, C.; Illas, F.; Caballol, R. *J. Phys. Chem*. A **2000**, *103*, 9983.
(10) Castell, O.; Caballol, R.; Miralles, J. *Chem. Phys* **1994**, *179*, 377.
(11) Illas, F.; Casanovas, J.; Garcia-Bach, M. A.; Caballol, R.; Castell,O. *Phys. Rev. Lett.* **1993**, *71*, 3549.
(12) Casanovas, J.; Illas, F. *J. Chem. Phys.* **1994**, *100*, 8257.
(13) Casanovas, J.; Illas, F. *J. Chem. Phys.* **1994**, *101*, 7683.
(14) de Graaf, C.; Illas, F.; Broer, R.; Nieuwpoort, W. C. *J. Chem. Phys.* **1997**, *106*, 3287.
(15) Moreira, I. de P. R.; Illas, F. *Phys. Rev. B* **1997**, *55*, 4129.
(16) Moreira, I. de P. R.; Illas, F. *Phys. Rev. B* **1999**, *60*, 5179.
(17) Reinhardt, P.; Habas, M. P.; Dovesi, R.; Moreira, I. de P. R.; Illas, F. *Phys. Rev. B* **1999**, *59*, 1016.
(18) Reinhardt, P.; Moreira, I. de P. R.; de Graaf, C.; Illas, F.; Dovesi, R. *Chem. Phys. Lett.* **2000**, *319*, 625.
(19) de Graaf, C.; Moreira, I. de P. R.; Illas, F.; Martin, R. L. *Phys. Rev. B* **1999**, *60*, 3457.
(20) Casanovas, J.; Rubio, J.; Illas, F. *Phys. Rev. B* **1996**, *53*, 945.
(21) Muñoz, D.; Illas, F.; Moreira, I. de P. R. *Phys. Rev. Lett.* **2000**, 84, 1579.
(22) Illas, F.; Moreira, I. de P. R.; de Graaf, C.; Castell, O.; Casanovas, J. *Phys. Rev. B* **1997**, *56*, 5069.

(23) Moreira, I. de P. R.; Illas, F.; Calzado, C. J.; Sanz, J. F.; Malrieu, J. P.; Ben Amor, N.; Maynau, D. *Phys. Rev. B* **1999**, *59*, R6593.
(24) Illas, F.; Moreira, I. de P. R.; de Graaf, C.; Barone, V. *Theor. Chem. Acc.* **2000**, *104*, 265.
(25) Bagus, P. S.; Bennet, B. I. *Int. J. Quantum Chem.* **1975**, *9*, 143.
(26) Ziegler, T.; Rauk, A.; Baerends, E. J. *Theor. Chim. Acta* **1977**, *43*, 261.
(27) Noodleman, L.; Norman, J. G., Jr. *J. Chem. Phys.* **1979**, *70*, 4903.
(28) Noodleman, L. *J. Chem. Phys.* **1981**, *74*, 5737.
(29) Noodleman, L.; Davidson, E. R. *Chem. Phys.* **1986**, *109*, 131.
(30) Noodleman, L.; Peng, C. Y.; Case, D. A.; Mouesca, J. M. *Coord. Chem. Rev.* **1995**, *144*, 199.
(31) Yamaguchi, K.; Fueno, T.; Ueyama, N.; Nakamura, A.; Ozaki, M. *Chem Phys. Lett.* **1989**, *164*, 210.
(32) Yamaguchi, K.; Tsunekawa, T.; Toyoda, Y.; Fueno, T. *Chem Phys. Lett.* **1988**, *143*, 371.
(33) Nagao, H.; Mitani, M.; Nishino, M.; Yoshioka, Y.; Yamaguchi, K. *Int. J. Quantum Chem.* **1997**, *65*, 947.
(34) Soda, T.; Kitagawa, Y.; Onishi, T.; Takano, Y.; Shigeta, Y.; Nagao, H.; Yoshioka, Y.; Yamaguchi, K. *Chem. Phys. Lett.* **2000**, *319*, 223.
(35) Ricart, J. M.; Dovesi, R.; Roetti, C.; Saunders: V. R. *Phys. Rev. B* **1995**, *52*, 2381; see also erratum in *Phys. Rev. B* **1997**, *55*, 15942.
(36) Bencini, A.; Totti, F.; Daul, C.; Doclo, K.; Fantucci, P.; Barone, V. *Inorg. Chem.* **1997**, *36*, 5022.
(37) Caballol, R.; Castell, O.; Illas, F.; Malrieu, J. P.; Moreira, I. de P. R. *J. Phys. Chem. A* **1997**, *101*, 7860.
(38) Adamo, C.; Barone, V.; Bencini, A.; Totti, F. Ciofini, I. *Inorg. Chem.* **1999**, *38*, 1996.
(39) Barone, V.; Bencini, A.; Ciofini, I.; Daul, C. *J. Phys. Chem. A* **1999**, *103*, 4275.
(40) Ruiz, E.; Alemany, P.; Alvarez, S.; Cano, S. *J. Am. Chem. Soc.* **1997**, *119*, 1297.
(41) Cano, J.; Alemany, P.; Alvarez, S.; Verdaguer, M.; Ruiz, E. *Chem. Eur. J.* **1998**, *4*, 476.
(42) Ruiz, E.; Alemany, P.; Alvarez, S.; Cano, J. *Inorg. Chem.* **1997**, *36*, 3683.
(43) Ruiz, E.; Cano, J.; Alvarez, S.; Alemany, P. *J. Comput. Chem.* **1999**, *20*, 1391.
(44) Becke, A. D. *J. Chem. Phys.* **1993**, *98*, 5648.
(45) Lee, C.; Yang, W.; Parr, R. G. *Phys. Rev. B* **1982**, *37*, 785.
(46) Barone, V.; Bencini, A.; di Matteo, A. *J. Am. Chem. Soc.*, **1997**, *119*, 10831.
(47) Martin, R. L.; Illas, F. *Phys. Rev. Lett.* **1997**, *79*, 1539.
(48) Illas, F.; Martin, R. L. *J. Chem. Phys.* **1998**, *108*, 2519.
(49) Pickett, W. E. *Rev. Mod. Phys.* **1989**, *61*, 433.
(50) Guo, G. Y.; Temmerman, W. M. *J. Phys. C* **1988**, *21*, L803.
(51) Mattheiss, L. F. *Phys. Rev. B* **1994**, *49*, 14050.
(52) Bader, R. F. W. *Atoms in Molecules: A Quantum Theory*; Oxford University Press: Oxford, 1990.
(53) Becke, A. D.; Edgecombe, K. E. *J. Chem. Phys.* **1990**, *92*, 5397.
(54) Silvi, B.; Savin, A. *Nature* **1994**, *371*, 683.
(55) Savin, A.; Nesper, R.; Wengert, S.; Fässler, T. P. *Angew. Chem. Int. Ed. Engl.* **1992**, *36*, 1809.
(56) Krokidis, X.; Noury, S.; Silvi, B. *J. Phys. Chem. A* **1997**, *101*, 7277.
(57) Noury, S.; Colonna, F.; Savin, A.; Silvi, B. *J. Mol. Struct.* **1998**, *450*, 59.
(58) Hart, J. R.; Rappé, A. K.; Gorum, S. M.; Upton, T. H. *J. Phys. Chem.* **1992**, *96*, 6264.
(59) Becke, A. D., *Phys. Rev. A* **1988**, *38*, 3098.
(60) Perdew, J. P.; Wang Y. *Phys. Rev. B* **1992**, *45*, 13244.
(61) Barone, V. In *Recent Advances in Density Functional Methods, Part I*; Chong, D. E., Ed.; World Scientific: Singapore, **1995**; p 287.
(62) Adamo, C.; Barone, V.; Fortunelli, A. *J. Chem. Phys.* **1995**, *102*, 384.
(63) Barone, V. *Theor. Chim. Acta* **1995**, *91*, 113.
(64) Adamo, C.; Barone, V. *J. Chem. Phys.* **1998**, *108*, 664.
(65) Adamo, C.; Barone, V. *J. Comput. Chem.* **1998**, *19*, 419.
(66) Frisch, M. J.; Trucks, G. W.; Schlegel, H. B.; Scuseria, G. E.; Robb, M. A.; Cheeseman, J. R.; Zakrzewski, V. G.; Montgomery Jr., J. A.; Stratmann, R. E.; Burant, J. C.; Dapprich, S.; Millam, J. M.; Daniels, A. D.; Kudin, K. N.; Strain, M. C.; Farkas, O.; Tomasi, J.; Barone, V.; Cossi, M.; Cammi, R.; Mennucci, B.; Pomelli, C.; Adamo, C.; Clifford, S.; Ochterski, J.; Petersson, G. A.; Ayala, P. Y.; Cui, Q.; Morokuma, K.; Malick, D. K.; Rabuck, A. D.; Raghavachari, K.; Foresman, J. B.; Cioslowski, J.; Ortiz, J. V.; Baboul, A. G.; Stefanov, B. B.; Liu, G.; Liashenko, A.; Piskorz, P.; Komaromi, I.; Gomperts, R.; Martin, R. L.; Fox, D. J.; Keith, T.; Al-Laham, M. A.; Peng, C. Y.; Nanayakkara, A.; Gonzalez, C.; Challacombe, M.; Gill, P. M. W.; Johnson, B.; Chen, W.; Wong, M. W.; Andres, J. L.; Gonzalez, C.; Head-Gordon, M.; Replogle, E. S.; Pople, J. A. *Gaussian 98*, Revision A.7; Gaussian, Inc.: Pittsburgh, PA, 1998.
(67) Noury, S.; Krokidis, X.; Fuster F.; Silvi, B. *TopMoD* package. www.lct.jussieu.fr (accessed 1997).
(68) Abraham, R. H.; Shaw, C. D. *Dynamics: The Geometry of Behavior*; Addisson Wesley: New York, 1992.
(69) Abraham, R. H.;. Marsden, J. E *Foundations of Mechanics*; Addison-Wesley: New York, 1994.
(70) Peixoto, M. *Topology* **1961**, *2*, 101.
(71) Palis, J.; Smale S. In *Proceedings of the Symposium on Pure Mathematics, XIV, Global Analysis*; American Mathematical Society: Providence, 1970; pp 223−231.
(72) Silvi, B.; Gatti, C. *J. Phys. Chem. A* **2000**, *104*, 947.
(73) Fuster, F.; Silvi, B. *Chem. Phys.* **2000**, *252*, 279.
(74) Stöll, H.; Pavlidou, C. M. E.; Preuss, H. *Theor. Chim. Acta* **1978**, *49*, 143.
(75) Colle, R.; Savetti, O. *Theor. Chim. Acta* **1979**, *53*, 55.
(76) Moscardó, F.; San-Fabián, E. *Int. J. Quantum Chem.* **1991**, *40*, 23.
(77) Pérez-Jordá, J. M.; San-Fabián, E.; Moscardó, F. *Phys. Rev. A* **1992**, *45*, 4407.
(78) Levy, M. *Proc. Natl. Acad. Sci. U.S.A.* **1979**, *76*, 6062.
(79) Illas, F.; Rubio, J.; Ricart, J. M.; Pacchioni, G. *J. Chem. Phys.* **1996**, *105*, 7192.
(80) Gill, P. M. W.; Johnson, B. G.; Pople J. A.; Frisch, M. J. *Int. J. Quantum Chem.* **1992**, *26*, 319.
(81) Willet R. In *Magneto Structutal Correlations in Exchange Coupled Systems*; Willet, R.; Gatteschi, D.; Kahn, O., Eds.; NATO-ASI Series C; Reidel: Dordrecht, 1985; p 140.
(82) Kasowski, R. V.; Tsai., M. H.; Dow, J. D. *Phys. Rev. B* **1990**, *41*, 7744.
(83) Hybertsen, M. S.; Stechel, E. B., Schluter, M.; Jennison, D. R. *Phys. Rev. B* **1990**, *41*, 11068.
(84) Steiner, M. M.; Albers, R. C.; Sham, L. J. *Phys. Rev. B* **1992**, *45*, 13272.
(85) Anisimov, V. I.; Korotin, M. A., Zaanen, J. A.; Anderson, O. K. *Phys. Rev. Lett.* **1992**, *68*, 345.
(86) Czyzyk, M. T.; Sawatzsky, G. A. *Phys. Rev. B* **1994**, *49*, 14211.
(87) Wei, P.; Qi, Z. Q. *Phys. Rev. B* **1994**, *49*, 12519.
(88) Svane, S. *Phys. Rev. Lett.* **1992**, *68*, 1900.
(89) Svane, S.; Gunnarsson, O. *Phys. Rev. Lett.* **1990**, *65*, 1148.